DTU Library

Global Frequency and Geographical Distribution of Nighttime Streamer Corona Discharges (BLUEs) in Thunderclouds

Soler, S.; GordilloVázquez, F. J.; PérezInvernón, F. J.; Luque, A.; Li, D.; Neubert, T.; Chanrion, O.; Reglero, V.; NavarroGonzález, J.; Østgaard, N.

Geophysical Research Letters®

Key Points:
- The first nighttime two-year climatology of streamer corona discharges (blue luminous events) in thunderclouds is presented
- Globally, the rate of blue luminous events at local midnight is ~11 per second
- Zonal and meridional distributions of blue luminous events peak in the northern tropic and the Americas, respectively

Supporting Information:
Supporting Information may be found in the online version of this article.

Correspondence to:
F. J. Gordillo-Vázquez,
vazquez@iaa.es

Global Frequency and Geographical Distribution of Nighttime Streamer Corona Discharges (BLUEs) in Thunderclouds

S. Soler[1] , F. J. Gordillo-Vázquez[1] , F. J. Pérez-Invernón[2] , A. Luque[1], D. Li[1], T. Neubert[3] , O. Chanrion[3] , V. Reglero[4], J. Navarro-González[4], and N. Østgaard[5]

[1]Instituto de Astrofísica de Andalucía (IAA-CSIC), Granada, Spain, [2]Deutsches Zentrum für Luft- und Raumfahrt, Institut für Physik der Atmosphäre, Weßling, Germany, [3]National Space Institute, Technical University of Denmark (DTU Space), Kongens Lyngby, Denmark, [4]Image Processing Laboratory, University of Valencia, Valencia, Spain, [5]Department of Physics and Technology, Birkeland Centre for Space Science, University of Bergen, Bergen, Norway

Abstract Blue LUminous Events (BLUEs) are transient corona discharges occurring in thunderclouds and characterized by strong 337.0 nm light flashes with absent (or weak) 777.4 nm component. We present the first nighttime climatology of BLUEs as detected by the Modular Multispectral Imaging Array of the Atmosphere-Space Interaction Monitor showing their worldwide geographical and seasonal distribution. A total (land and ocean) of ~11 BLUEs occur around the globe every second at local midnight and the average BLUE land/sea ratio is ~7:4. The northwest region of Colombia shows an annual nighttime peak. Globally, BLUEs are maximized during the boreal summer-autumn, contrary to lightning which is maximed in the boreal summer. The geographical distribution of nighttime BLUEs shows three main regions in, by order of importance, the Americas, Europe/Africa and Asia/Australia.

Plain Language Summary Blue LUminous Events (BLUEs) are transient corona discharges occurring in thunderclouds and characterized by their distinct 337.0 nm light flashes with absent (or negligible) 777.4 nm component. We present the first two year nighttime climatology of BLUEs as detected by the Modular Multispectral Imaging Array of the Atmosphere-Space Interaction Monitor on board the International Space Station that shows distinct worldwide geographical and seasonal distributions.

1. Introduction

Different observational evidence over the last 40 years suggests that cold, non-thermal streamer corona discharges are common in thunderstorms around the globe (Bandara et al., 2019; Le Vine, 1980; Neubert et al., 2021; Soler et al., 2020; Wiens et al., 2008). Fast breakdown (Rison et al., 2016; Tilles et al., 2019) suggests streamer coronas to be the cause of narrow bipolar events (NBEs). NBEs were originally detected by Le Vine (1980) in the form of strong radio frequency sources from in-cloud electrical activity. Such sources were characterized by short-duration (10–30 μs) bipolar sferic waveforms recorded in the very low frequency (VLF)/low frequency (LF) (10–400 kHz) range (Smith et al., 1999). NBEs can also appear accompanied by strong very high frequency (VHF) (30–300 MHz) radiation bursts.

In terms of light emissions, both impulsive and continuous streamer corona discharges in air are distinctly characterized by spectra strongly dominated by near-ultraviolet blue emissions (300–450 nm) corresponding to the Second Positive System (SPS) of molecular nitrogen (N_2) (Ebert et al., 2010; Gallimberti et al., 1974; Grum & Costa, 1976) with its strongest transition in 337.0 nm (Gordillo-Vázquez et al., 2012; Hoder et al., 2016, 2020; Malagón-Romero & Luque, 2019). Available laboratory measurements also show that red and near-infrared optical features from the First Positive System (FPS) of N_2 and the spectral contribution from oxygen atoms is negligibly small (0.5%–4%) compared to N_2 SPS in both leader and leaderless streamer coronas (Ebert et al., 2010; Gallimberti et al., 1974; Grum & Costa, 1976). Finally, leader coronas spectra exhibit larger (double) intensity of N_2^+ First Negative System (FNS) at 391.4 nm than leaderless corona discharges (Gallimberti et al., 1974).

Transient (from a few to hundreds of milliseconds) bluish optical emissions from thunderstorm cloud tops were originally identified from aircraft by Wescott et al. (1995, 1996). They distinguished two types, fast

upward moving jets named blue jets reaching terminal heights of 45–50 km (Wescott et al., 1995), and blue starters that protrude upward from the cloud top to a maximum of ~25 km and that were not coincident with negative or positive cloud to ground (CG) lightning strokes (Wescott et al., 1996). Multispectral video recordings show evidence that a small fraction of bluish optical emissions from both blue jets and starters are due to N_2^+ FNS (Wescott et al., 2001).

The term Blue LUminous Events (BLUEs) can then be safely applied to in-cloud and to (partially) emerged transient electrical discharges that emit pulses of light mostly blue, that is, it could include a small fraction of red and infrared optical emissions (600–900 nm). This definition includes blue jets and starters, but also positive and negative NBEs, which are the VLF/LF radio manifestation of in-cloud streamer coronas (Cooray et al., 2020; Li et al., 2021; Liu et al., 2018; N. Liu et al., 2019; Rison et al., 2016; Soler et al., 2020; Tilles et al., 2019).

Optical detection of BLUEs has been increasingly efficient since the beginning of the XXI century. During the Severe Thunderstorm Electrification and Precipitation Study ground-based campaign in 2000 (Lyons et al., 2003), brief (33–136 ms) up-propagating discharges called *gnomes* were filmed slightly (~1 km) rising out of the convective dome of a supercell storm in the Great Plains of the United States. In 2011, also from the ground, Edens (2011) reported a real color image with associated in-cloud VHF sources of a small blue starter that occurred on August 4, 2010 over an active thunderstorm in west central New Mexico. The event exhibited three diffuse streamer regions attached to leader-like channels, which appeared more white in the color image than the blue streamers emerging from the cloud top at ~15 km and reaching a terminal altitude of ~17 km (Edens, 2011).

Optical BLUE detections from space have been reported from the limb-pointing Imager of Sprites/Upper Atmospheric Lightning (ISUAL) onboard FORMOSAT-2 (Chou et al., 2011, 2018; Kuo et al., 2005, 2015; Liu et al., 2018). Chou et al. (2018) reported dim red emissions (623–754 nm) at the lower edge of some ISUAL detected BLUEs. A variety of BLUEs including kilometer-scale blue discharges at the cloud top layer at ~18 km altitude, blue starters and a pulsating blue jet propagating into the stratosphere were color photographed from the International Space Station (ISS) (Chanrion et al., 2017). BLUEs have also been recently observed by the nadir-pointing Modular Multispectral Imaging Array (MMIA) onboard Atmosphere-Space Interaction Monitor (ASIM) in the ISS since April 2018 (Li et al., 2021; Neubert et al., 2021; Soler et al., 2020).

By compositing 2 years of BLUEs data recorded by the MMIA instrument of ASIM on-board the ISS (Neubert et al., 2019) we present the first worldwide nighttime climatology of BLUEs in thunderclouds. We discuss key aspects such as average annual and seasonal distribution, regional differences, land/ocean variability, zonal/meridional distributions, and the global rate of BLUEs in local time.

2. Observations and Data

Observations of BLUEs were done with the MMIA high sampling rate (100 kHz) photometers in the near UV (337 nm/4 nm), tuned to the strongest line of the N_2 SPS, and in the near infrared band (777.4 nm/5 nm) for recording the atomic oxygen triplet line of lightning strokes. MMIA also incorporates a high-speed photometer in the UV (180–230 nm) recording part of the N_2 Lyman-Birge-Hopfield band, and a pair of 337 nm/4 nm and 777.4 nm/5 nm filtered cameras (at 12 fps) with ~400 m/pixel spatial resolution (Chanrion et al., 2019). An important boundary condition of this study is that MMIA observes only during nighttime.

BLUEs exhibit strong features in the 337 nm/4 nm photometer with negligible (barely above the noise level 0.4 μW/m^2) signal in the 777.4 nm/5 nm photometer, which is also continuously monitored. Once a true positive BLUE detection is confirmed, the cameras are checked for possible associated images. The climatology now presented was built with two years of worldwide MMIA level 1 (calibrated) data covering the period from September 1, 2018 to August 31, 2020.

Due to the inclination (~52°) of the ISS orbit, locations near the equator are observed less frequently than those in higher latitudes. When calculating the average global rate of BLUEs from MMIA data, the number and location of BLUE flashes observed by MMIA were computed using the observation time of MMIA (see Text S1 and Figure S1). The surface of the Earth was divided into 2° × 2° grid cells for the annual (and
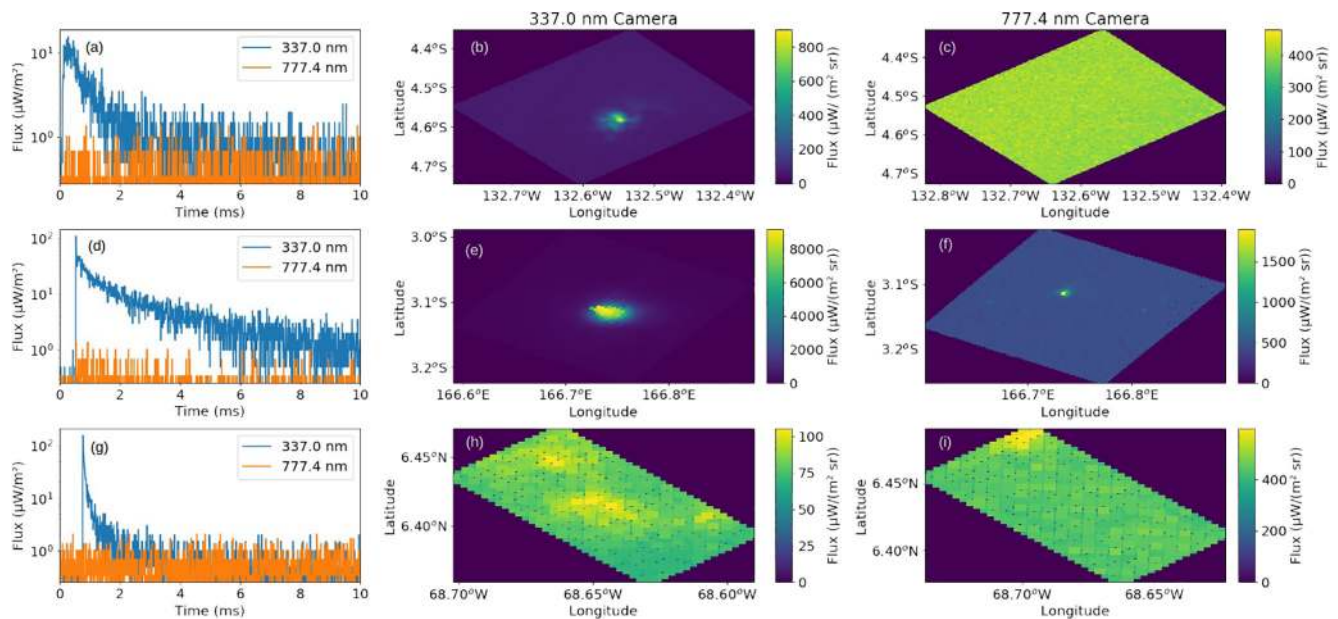
Figure 1. Three representative types of Blue LUminous Events (BLUEs) investigated in this global study. The top, middle and bottom panels display the temporal shape, (a, d, g) duration and intensity of the 337.0 and 777.4 nm photometer light curves, and the associated BLUE images in the (b, e, h) 337.0 nm and (c, f, i) 777.4 nm cameras (with 400 m pixel resolution). The impulsive behavior of the 337.0 nm is clearly seen in the three cases while noise level signals are simultaneously detected in the 777.4 nm photometer and camera of common BLUEs (a, b, c and g, h, i panels). The (d, e, f) panels present the case of a possible Blue Starter, which include measurable 777.4 nm signals due to its leader and a 337.0 nm camera image that is saturated. The 337.0 nm light (photometer) curve of the Blue Starter hardly lasts beyond 4 ms, while the duration of the 777.4 nm light curve is about 2 ms. The three BLUEs shown occurred (from top to bottom) on April 14, 2019 at 04:49:41 UTC, Feb 26, 2019 15:10:41 UTC and July 23, 2019 at 08:15:36 in Lon, Lat (131.25°W, 4.99°S) middle of Pacific ocean, (164.60°E, 3.11°S) east of Solomon Islands, and (67.58°W, 6.01°N) north of Puerto Ayacucho in Colombia very close to the border with Venezuela, respectively.

seasonal) geographical distributions and into $1° \times 1°$ grid cells for the annual cycle of global BLUE rate in terms of zonal and meridional distributions.

Figure 1 shows the appearance of three representative cases of BLUEs investigated in this global study. The top, middle and bottom panels display the temporal shape, duration and intensity of the 337.0 and 777.4 nm photometer light curves (left column), and the associated images in the 337.0 nm (central colum) and 777.4 nm (right column) filtered cameras. The impulsive behavior of the 337.0 nm is clear in the three cases with peak values (and durations), from top to bottom, of ~15 μW/m^2 (~2 ms), ~110 μW/m^2 (~4 ms) and ~150 μW/m^2 (~0.3 ms). The 777.4 nm component is negligible in BLUEs displayed in the top and bottom panels, which according to their 337.0 nm light curve shape corresponds to the optical manifestation of positive (top) and negative NBEs (bottom). The event in the middle panel could be a Blue Starter exhibiting a weak (but measurable) 777.4 camera signal due to an upward moving leader.

3. Methodology

As presented in the introduction, based on what it is known about optical emissions of leaders and streamer coronas (Li et al., 2021; Neubert et al., 2021; Soler et al., 2020), and of MMIA photometer sensitivity and noise levels (Chanrion et al., 2019), an algorithm for identification of BLUEs was designed. The algorithm analyzed all the 337 nm/4 nm (blue) and 777.4 nm/5 nm (red) photometer events recorded by MMIA in the period of study. A photometer event is composed of a number N of frames (usually between 3 and 8) with a duration of ~83 milliseconds each. The algorithm relies on seven sequential steps that analyze the concatenated frames of an event.

(1) Consider only frames of photometer events with "phot1trigger=1" (trigger of 337.0 nm photometer) regardless of other MMIA photometer triggers (details of triggering modes and MMIA-MXGS cross-triggering can be found in Chanrion et al. (2019)). (2) Given a photometer event, calculate the blue and red

median values in each frame. Compute the blue and red thresholds by adding 3σ to, respectively, the means of the blue and red values below the corresponding medians. (3) If threshold values are below 1 μW/m^2, as they are commonly found, they are replaced by 1 μW/m^2 (about two or three times the noise level of the red and blue photometers). (4) Create groups defined by five or more consecutive blue counts (10 μs each) above the blue threshold. Groups separated by more than 10 milliseconds are considered different single BLUE events. (5) Given groups of blue counts, find the maximum (or peak) in each group and keep only the groups with no red sequence (above the red threshold) 15 and 5 milliseconds before and after the blue peak, respectively. (6) Disregard very weak BLUEs by requesting that the maximum blue signal is at least 3 times the blue threshold. (7) Given groups of blue counts with red signal, keep only those events for which: (a) the red peak is above 2.5 μW/m^2 and the blue maximum is at least 10 times the red peak or, (b) the red peak is below or equal 2.5 μW/m^2 and the blue maximum is at least 2 times the red peak. Note that 2.5 μW/m^2 was chosen as the red border value because the red signal can start to be noisy below it.

In general and in order to minimize the number of false positives, the algorithm also removes all photometer events with or without Modular X and Gamma ray Sensor (MXGS) trigger but no MMIA trigger, both outside and over the South Atlantic Anomaly (SAA) where MMIA also operates. Note that steps 5 and mostly 7 of the algorithm already filter out a lot of false positive BLUE events in the SAA where energetic particles can trigger the photometers and usually appear in the blue and red photometers as sharp and randomly distributed events.

4. Results

Worldwide BLUE geographical distributions are shown in Figures 2, 3, and 4 for annual and seasonal averages, respectively. Because of the relatively short period analyzed (two years), the BLUE density maps are not fully smooth because of sampling limitations. We detected a total of about 53015 nighttime BLUEs within the ASIM-MMIA FOV. During nighttime only, ISS-LIS detected about 1.04M lightning flashes. Since ISS-LIS FOV is 2.56 times larger than MMIA FOV, we have that, during nighttime, ISS-LIS/MMIA = 1.04M/ (0.053M × 2.56) = 7.7.

4.1. Global Annual and Zonal/Meridional Distributions

The worldwide annual average (Figure 2a) exhibit high activity BLUE spots in northern Colombia/Lake Maracaibo region (Venezuela), Peru/Bolivia border, northwestern Brazil, central Africa, northeastern Himalaya, Bangladesh and northeastern Malaysia. BLUE flash rate densities peak over northern Colombia (Santa Marta region) with values of ~ 30 BLUEs km^{-2} year^{-1} (provided night and day have the same global flash rate), rather than in central Africa (with 18 BLUEs km^{-2} year^{-1}) as occur with lightning flashes (Blakeslee et al., 2020; Christian et al., 2003).

The clear bimodal peak in the zonal distribution of nighttime lightning flashes detected by the Lightning Imager Sensor (LIS) onboard the ISS (gray line in Figure 2c) is not exhibited in the zonal distribution of BLUEs, which presents an uneven three-peak equatorial structure with the highest peak in the northern tropic (blue line in Figure 2c). The meridional distribution of BLUEs (blue line in Figure 2b) clearly shows three active chimneys in the Americas, Europe/Africa, and Asia/Australia. There is a fourth chimney slightly visible around 150°W-15°S near Tahiti in Figures 2a and 3c during MAM (see also Figure S11). While the nighttime lightning meridional distribution presents the largest (and sharp) peak in Europe/Africa as shown in Figure 2b (gray line), the net contribution of BLUEs from the Americas is larger than those in the other two regions (see blue line in Figure 2b).

The comparison between the annual average zonal distributions of BLUEs and nighttime lightning shows that the contribution of the tropical region between 20°S to 20°N latitude is almost a factor 3 to 4 that of the subtropics for BLUEs, while it is a factor ~2 for lightning, which indicates a faster (than nighttime lightning flash rate) decrease of the BLUE rate towards higher latitudes. This suggests that deeper storms give a lot more BLUEs and NBEs (C. Liu et al., 2007; Suszcynsky & Heavner, 2003). We have used the convective available potential energy (CAPE), a reasonable good proxy of deep convection (Ukkonen & Mäkelä, 2019;
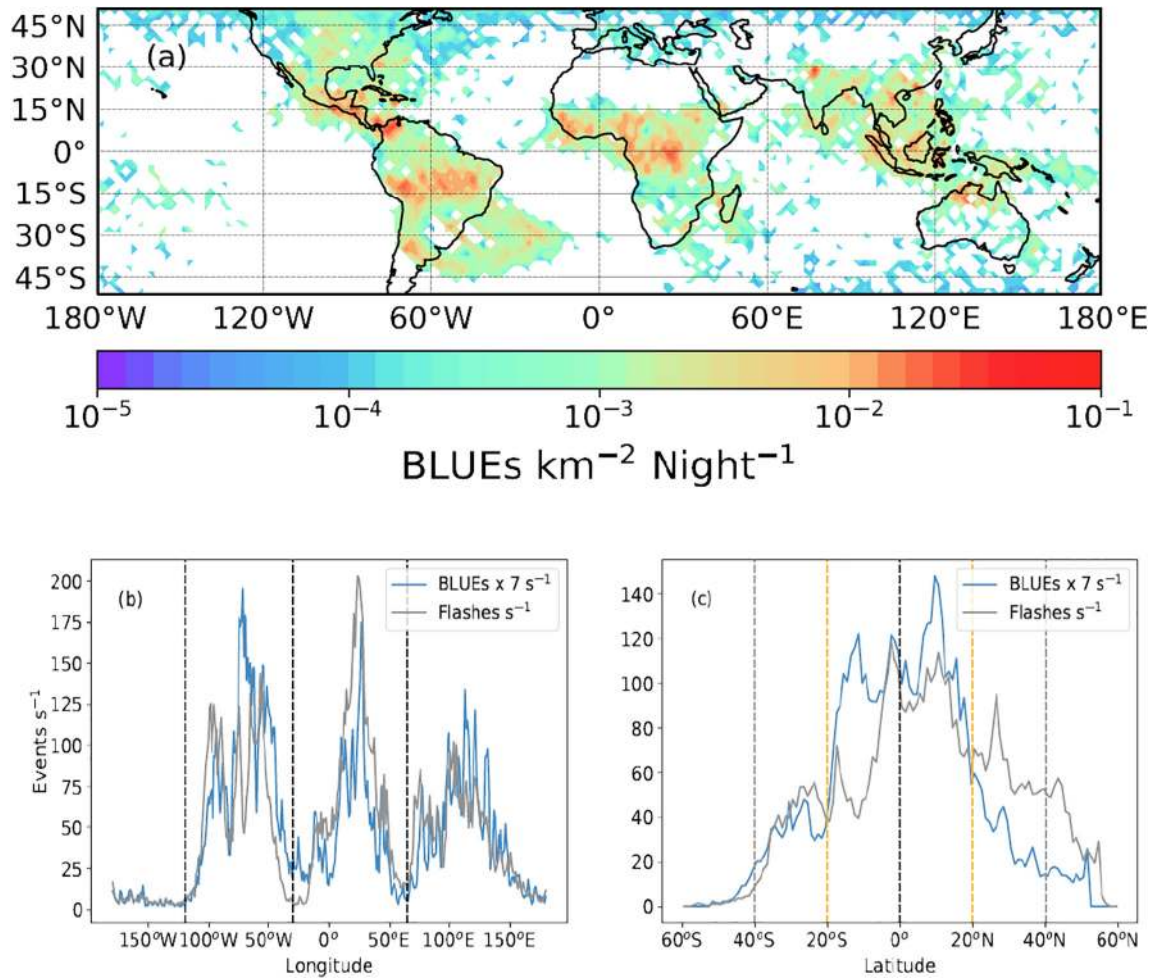
Figure 2. Panel (a): Two-year average (September 2018 through August 2020) nighttime climatology of global Blue LUminous Event (BLUE) electrical activity in thunderclouds. The map is generated using $2° \times 2°$ grid cells where the sharp pixels of the image are smoothed by drawing level lines using the python function called *contourf*. Decimal logarithm is used in the colorbar scale so that 0.08 (roughly the maximum in the map) corresponds to ~30 BLUEs km^{-2} $year^{-1}$ provided night and day have the same global flash rate. Panels (b, c): Annual cycle (for the period investigated) of ASIM-MMIA nighttime global BLUE flash rate (blue line) and ISS-LIS global nighttime flash rate (gray line) represented in meridional (b) and zonal (c) distributions. Three BLUE and nighttime lightning chimneys are clearly distinguishable in the Americas (120°W-25°W), Africa/Europe (25°W-60°E) and Asia/Australia (60°E-180°E) in the meridional distributions. There is a fourth chimney slightly visible around 150°W-15°S near Tahiti. Tropical (20°S-20°N), subtropical (40°S-20°S, 20°N-40°N) and midlatitude (60°S-40°S, 40°N-60°N) regions are indicated in the zonal distributions with dashed orange and gray vertical lines, respectively. The (b) and (c) panels were generated using $1° \times 1°$ grid cells. A non smooth two-year average nighttime climatology map of BLUEs is shown in Figure S10. Note that the global BLUE rates are scaled up 7 times for best comparison with global nighttime lightning flash rates.

Williams et al., 1992), to quantify the possible linear relationship between BLUEs and deep convection (see Figure S12).

4.2. Global Seasonal, Zonal/Meridional Distributions and Local Time Variability

The seasonal nighttime average distribution of BLUEs shown in Figure 3 indicates that the global BLUE electrical activity peaks during the boreal autumn (8.2 (SON), 5.9 (DJF), 6.2 (MAM) and 6.7 (JJA) BLUEs s^{-1}) while lightning peak in the boreal summer (see Figures S4 and S7). The boreal summer and spring seasons also display important worldwide BLUE activity. The months of December-February have little BLUE activity in the Northern Hemisphere that, instead, concentrates in southern America, austral Africa, Indonesia and northern Australia. The central and northern Great Plains, the Tornado alley of the United States and the Mediterranean Europe exhibit their greatest nighttime BLUE activity in the boreal fall. The Lake Maracaibo region exhibits high BLUE activity all year long except during December-February. Most
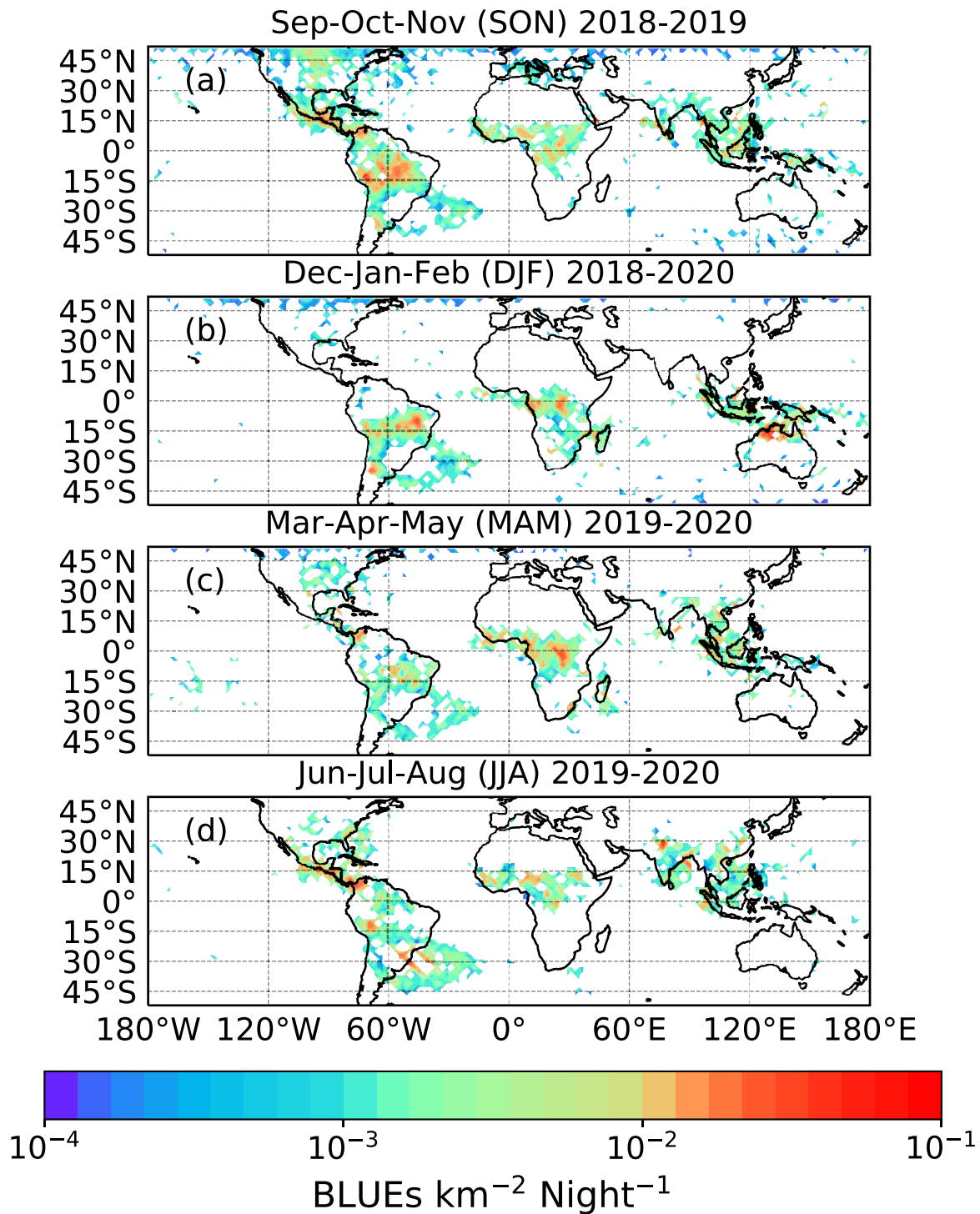
Figure 3. Nighttime seasonal distribution of Blue LUminous Event (BLUE) electrical activity in thunderclouds. The global nighttime seasonal BLUE rates are: 8.2 (SON), 5.9 (DJF), 6.2 (MAM) and 6.7 (JJA) BLUEs s^{-1}. Note that these global nighttime seasonal BLUE rates are biased (underestimated) due to the nighttime only ASIM-MMIA observation time mode (see Figure 5) that shortens as ISS moves since it is not a geostationary platform. Thus, the most representative nighttime BLUE rate would be that at 0 h local time (see Figure 5). These maps are generated using 2° × 2° grid cells where the sharp pixels of the image are smoothed by drawing level lines using the python function called *contourf*. Note that decimal logarithm is used in the colorbar. Non smooth seasonal maps are shown in Figure S11.
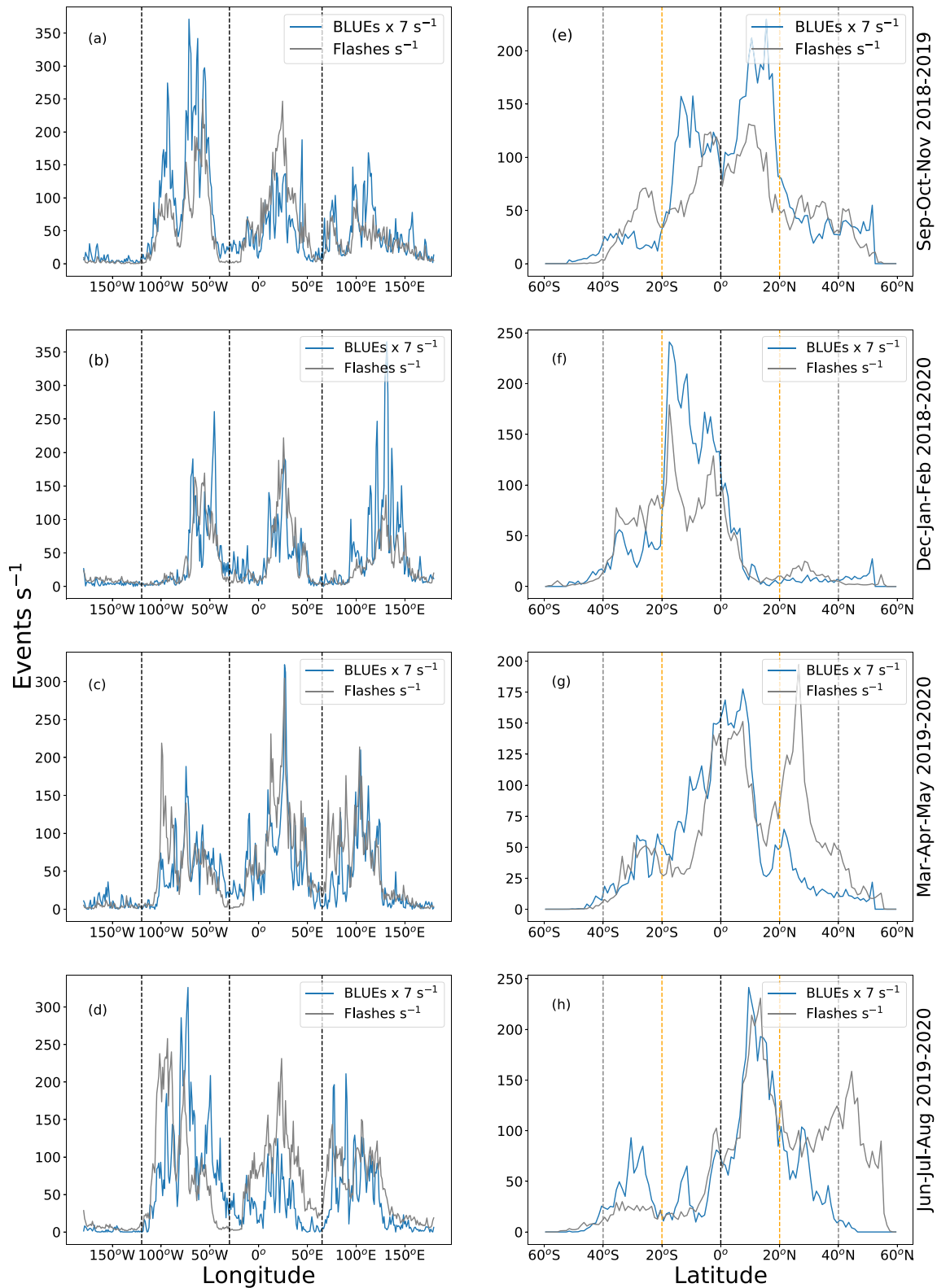
Figure 4. Seasonal meridional (left) and zonal (right) nighttime distributions of 2-year (September 1, 2018 to August 31, 2020) Blue LUminous Event climatology and ISS-LIS nighttime lightning in the same period. Grid cells and vertical lines as in Figure 2. Note that, for comparison, seasonal meridional/zonal 24 h (day and night) distribution of the two-year ISS-LIS lightning climatology is shown in Figure S8. Note that the global seasonal BLUE rates are scaled up 7 times for best comparison with global nighttime lightning flash rates.
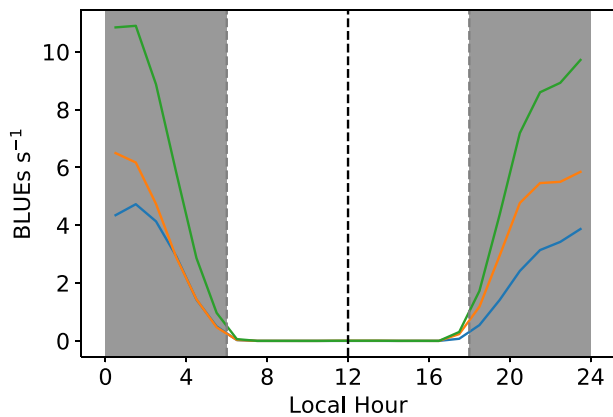
Figure 5. Diurnal (24 h) variability of global total (green line), land (orange line) and ocean (blue line) Blue LUminous Event flash rate as a function of the local solar hour. The net zero rate during local daytime is caused by the fact that ASIM-MMIA can only observe during local nighttime. Local nighttime periods appear shadowed in the figure. Note that, for comparison, Figure S9 shows the diurnal (day and night) cycle of ISS-LIS total, land and ocean lightning flash rates for the two-year period investigated.

BLUEs in the Indian subcontinent and the Bay of Bengal occur during the monsoon season from early June to the beginning of October. BLUEs in the pre-monsoon period (MAM) are also distinguishable in the Bay of Bengal (see Figure 3c). The nature of convection is very different in the pre-monsoon and break period, and the real monsoon season shown in Figure 3d (Williams et al., 1992). See Figure S12 and further comments in the Supporting Information S1.

The very weak BLUE activity along the United States/Canada border (a pyroconvection region) extending to eastern and western regions in the 45°N-52°N latitude band, from the boreal autumn to spring, could be related to the United States/Canada fire season (April-October) when plenty of pyrocumulus and pyrocumulonimbus are formed (Fromm et al., 2010). However, the fact that there is no BLUE activity in the boreal summer months in that region suggests that BLUEs in that region could be connected instead with boreal winter lightning (Montanyà et al., 2016), which are negligible in the US/Canada border during the boreal summer. Similarly, bushfire season in Australia (with significant pyroconvection activity) normally starts in July/August and extends up to March (Dowdy & Pepler, 2018) partially overlapping with the austral winter lightning season (June-August). On the other hand, the unusually intense 2019/2020 bushfire season peaked in austral summer (December 2019/January 2020) (Y. Liu et al., 2021; Schwartz et al., 2020) with some (but very weak) overlapping BLUE activity to the south of Australia, which might indicate a possible BLUE connection with Australian bushfires (plus a possible austral autumn-winter lightning component).

Figure 4 presents the seasonal meridional (left column) and zonal (right column) nighttime distributions of the 2-year BLUE climatology (blue line) and ISS-LIS nighttime lightning (gray line). According to the meridional representation, the largest BLUE (and nighttime lightning) chimney is in the Americas during the boreal autumn and summer, but the largest BLUE chimney shifts to Asia/Australia and Europe/Africa in the boreal winter and spring, respectively. This behavior slightly differs from that of the boreal winter and spring nighttime lightning meridional distributions, which present their largest chimney in the Europe/Africa (mostly Africa) region. The fact that the Northern hemisphere has 68% of the Earth's land by area shapes the BLUE and nighttime lightning seasonal zonal distributions. BLUEs and nighttime lightning only dominate in Southern Hemisphere during the austral summer.

As shown in Figure 5, on average, BLUEs peak at ~11 flashes s^{-1} in the local midnight (00.00 local solar time), and show a decreasing global rate as local daytime approaches (and there is less MMIA observation time) characterized by a sharper slope than nighttime lightning flash rate (see Figure S9) for the same period. BLUEs exhibit a local midnight land/sea ratio of ~7:4 (for ~3:1 for lightning).

5. Discussion and Conclusions

The ASIM-MMIA nighttime climatology of BLUEs presented in this paper is the first of its kind and complements the global frequency and 24 h lightning distribution (within ± 70° latitude) first available since 2003 (Christian et al., 2003). This was generated with data from the Optical Transient Detector, a prototype of LIS, in operation from May 1995 to March 2000. LIS was later onboard the Tropical Rainfall Measuring Mission (TRMM) also providing full day global lightning data within ± 38° latitude from early 1998 to April 2015 when TRMM was deorbited (Cecil et al., 2014). More recently, since March 1, 2017, LIS is onboard the ISS providing high latitude (up to ± 52°) all-day (24 h) lightning data (Blakeslee, 2019; Blakeslee et al., 2020).

Research results through the last 40 years indicate that, in addition to lightning, kilometer scale corona electrical discharges formed by hundreds of millions of streamers (Cooray et al., 2020; Li et al., 2021; N. Liu et al., 2019) are common in thunderclouds around the globe but their genesis (Le Vine, 1980; Neubert et al., 2021; Rison et al., 2016; Smith et al., 1999; Soler et al., 2020; Tilles et al., 2019), dynamics (Bandara et al., 2019, 2021; Jacobson & Heavner, 2005; Jacobson et al., 2013; Wiens et al., 2008) and probable

atmospheric chemistry impact (Bozem et al., 2014; Gordillo-Vázquez & Pérez-Invernón, 2021; Minschwaner et al., 2008; Pérez-Invernón et al., 2019; Shlanta & Moore, 1972; Simek, 2002; Zahn et al., 2002) remain to be well understood.

While the hot and thermal lightning plasma mostly excites atomic species like oxygen atoms released from thermal dissociation of O_2 leading to 777.4 nm optical emissions typical of lightning, streamer corona discharges are cold non-thermal plasmas where only heavy particles are cold and electrons are very hot. Thus corona discharges are able to activate molecular species like N_2, O_2 and H_2O by non-equilibrium electron-impact collisions (Gordillo-Vázquez et al., 2018). This underlies their different efficiencies in producing key chemical species. For instance, lightning is a key direct source of tropospheric nitride oxide (NO) that, when oxidized, produces NO_2 leading to the known lightning NO_x (LNO_x) with significant impact on tropospheric chemistry (Gordillo-Vázquez et al., 2019; Finney et al., 2016; Schumann & Huntrieser, 2007). In contrast, laboratory produced streamer coronas generate only small amounts of NO but considerable greenhouse gases such as ozone (O_3) and nitrous oxide (N_2O) (Brandvold et al., 1996; Donohoe et al., 1977), which is an ozone depleting gas and the third strongest greenhouse gas after carbon dioxide and methane. N_2O has the largest (~300 times that of CO_2 for a 100-year timescale) global warming potential of these gases (Myhre et al., 2014). Perturbations to concentrations of greenhouse gases affect the radiation balance more the higher the altitude of the sources. In this respect ASIM can facilitate their detection since it is more sensitive to discharges higher in the clouds.

The present results suggest that streamer corona discharges in thunderclouds are relatively common as observed by ASIM-MMIA. Thus, thundercloud streamer corona discharges, which can occur continuously in the vicinity of ordinary lightning strokes, but also in isolation, may be a critical upper troposphere source of greenhouse gases such as N_2O and O_3, and of oxidant gases like OH and HO_2, in convectively active areas that deserves further detailed studies.

Our global and seasonal nighttime thundercloud streamer corona distributions, zonal and meridional averages, and nighttime variability provide the first worldwide view of coronas occurring in thunderstorms. These results can set the path for future studies that should deepen our knowledge on key themes such as types of corona discharges in thunderclouds, morphology (and dynamics) of optical (and radio) emissions from the heads and long-lasting glows of streamers in thundercloud coronas (Luque et al., 2016; Pérez-Invernón et al., 2020), role of meteorological conditions (F. Liu et al., 2021) in favoring their initiation/deactivation (Huang et al., 2021) and, finally but no less important, to explore the impact of non-equilibrium (electron driven) chemical reactions triggered by hundreds of millions of streamers in kilometer long cloud coronas (Brune et al., 2021; Gordillo-Vázquez & Pérez-Invernón, 2021) on the atmospheric chemistry of the upper troposphere and lower stratosphere.

Data Availability Statement

ASIM level 1 data are proprietary and cannot be publicly released at this stage. Interested parties should direct their request to the ASIM Facility Science Team (FST). ASIM data request can be submitted through: https://asdc.space.dtu.dk by sending a message to the electronic address asdc@space.dtu.dk. ISS-LIS data in https://ghrc.nsstc.nasa.gov/lightning/data/data_lis_iss.html are freely accessed from the NASA Global Hydrology Resource Center.

References

Bandara, S., Marshall, T., Karunarathne, S., Karunarathne, N., Siedlecki, R., & Stolzenburg, M. (2019). Characterizing three types of negative narrow bipolar events in thunderstorms. *Atmospheric Research*, *227*, 263–279. https://doi.org/10.1016/j.atmosres.2019.05.013

Bandara, S., Marshall, T., Karunarathne, S., & Stolzenburg, M. (2021). Groups of narrow bipolar events within thunderstorms. *Atmospheric Research*, *252*, 105450. https://doi.org/10.1016/j.atmosres.2021.105450

Blakeslee, R. (2019). *Non-quality controlled lightning imaging sensor (LIS) on international space station (ISS) science data*. NASA Global Hydrology Resource Center DAAC: Huntsville, AL, USA. https://doi.org/10.5067/LIS/

Blakeslee, R. J., Lang, T. J., Koshak, W. J., Buechler, D., Gatlin, P., Mach, D. M., & et al. (2020). Three years of the lightning imaging sensor onboard the international space station: Expanded global coverage and enhanced applications. *Journal of Geophysical Research: Atmospheres*, *125*(16), e2020JD032918. https://doi.org/10.1029/2020jd032918

Bozem, H., Fischer, H., Gurk, C., Schiller, C., Parchatka, U., Koenigstedt, R., et al. (2014). Influence of corona discharge on the ozone budget in the tropical free troposphere: A case study of deep convection during gabriel. *Atmospheric Chemistry and Physics*, *14*(17), 8917–8931. https://doi.org/10.5194/acp-14-8917-2014

Brandvold, D. K., Martinez, P., & Hipsh, R. (1996). Field measurements of O_3 and N_2O produced from corona discharge. *Atmospheric Environment*, *30*(6), 973–976. https://doi.org/10.1016/1352-2310(95)00234-0

Brune, W., McFarland, P., Bruning, E., Waugh, S., MacGorman, D., Miller, D., & Peischl, J. (2021). Extreme oxidant amounts produced by lightning in storm clouds. *Science*, *372*, 711–715. https://doi.org/10.1126/science.abg0492

Cecil, D. J., Buechler, D. E., & Blakeslee, R. J. (2014). Gridded lightning climatology from trmm-lis and otd: Dataset description. *Atmospheric Research*, *135*, 404–414. https://doi.org/10.1016/j.atmosres.2012.06.028

Chanrion, O., Neubert, T., Mogensen, A., Yair, Y., Stendel, M., Singh, R., & Siingh, D. (2017). Profuse activity of blue electrical discharges at the tops of thunderstorms. *Geophysical Research Letters*, *44*(1), 496–503. https://doi.org/10.1002/2016gl071311

Chanrion, O., Neubert, T., Rasmussen, I. L., Stoltze, C., Tcherniak, D., Jessen, N. C., et al. (2019). The Modular Multispectral Imaging Array (MMIA) of the ASIM payload on the International Space Station. *Space Science Reviews*, *215*(4), 28. https://doi.org/10.1007/s11214-019-0593-y

Chou, J., Tsai, L., Kuo, C., Lee, Y., Chen, C., Chen, A., & Lee, L. (2011). Optical emissions and behaviors of the blue starters, blue jets, and gigantic jets observed in the Taiwan transient luminous event ground campaign. *Journal of Geophysical Research*, *116*(A7), A07301. https://doi.org/10.1029/2010ja016162

Chou, J.-K., Hsu, R.-R., Su, H.-T., Chen, A. B.-C., Kuo, C.-L., Huang, S.-M., et al. (2018). ISUAL-observed blue luminous events: The associated sferics. *Journal of Geophysical Research: Space Physics*, *123*(4), 3063–3077. https://doi.org/10.1002/2017ja024793

Christian, H. J., Blakeslee, R. J., Boccippio, D. J., Boeck, W. L., Buechler, D. E., Driscoll, K. T., & et al. (2003). Global frequency and distribution of lightning as observed from space by the Optical Transient Detector. *Journal of Geophysical Research*, *108*(D1), 4005. https://doi.org/10.1029/2002jd002347

Cooray, V., Cooray, G., Rubinstein, M., & Rachidi, F. (2020). Modeling compact intracloud discharge (CID) as a streamer burst. *Atmosphere*, *11*(5), 549. https://doi.org/10.3390/atmos11050549

Donohoe, K. G., Shair, F. H., & Wulf, O. R. (1977). Production of O_3, NO, and N_2O in a pulsed discharge at 1 atm. *Industrial & Engineering Chemistry Fundamentals*, *16*(2), 208–215. https://doi.org/10.1021/i160062a006

Dowdy, A. J., & Pepler, A. (2018). Pyroconvection risk in Australia: Climatological changes in atmospheric stability and surface fire weather conditions. *Geophysical Research Letters*, *45*(4), 2005–2013. https://doi.org/10.1002/2017gl076654

Ebert, U., Nijdam, S., Li, C., Luque, A., Briels, T., & van Veldhuizen, E. (2010). Review of recent results on streamer discharges and discussion of their relevance for sprites and lightning. *Journal of Geophysical Research*, *115*, A00E43. https://doi.org/10.1029/2009JA014867

Edens, H. (2011). Photographic and lightning mapping observations of a blue starter over a New Mexico thunderstorm. *Geophysical Research Letters*, *38*(17), L17804. https://doi.org/10.1029/2011gl048543

Finney, D., Doherty, R., Wild, O., & Abraham, N. L. (2016). The impact of lightning on tropospheric ozone chemistry using a new global lightning parametrisation. *Atmospheric Chemistry and Physics*, *16*(12), 7507–7522. https://doi.org/10.5194/acp-16-7507-2016

Fromm, M., Lindsey, D. T., Servranckx, R., Yue, G., Trickl, T., Sica, R., & Godin-Beekmann, S. (2010). The untold story of pyrocumulonimbus. *Bulletin of the American Meteorological Society*, *91*(9), 1193–1210. https://doi.org/10.1175/2010bams3004.1

Gallimberti, I., Hepworth, J. K., & Klewe, R. C. (1974). Spectroscopic investigation of impulse corona discharges. *Journal of Physics D: Applied Physics D*, *7*, 880–898. https://doi.org/10.1088/0022-3727/7/6/315

Gordillo-Vázquez, F. J., Luque, A., & Simek, M. (2012). Near infrared and ultraviolet spectra of TLEs. *Journal of Geophysical Research*, *117*, A05329. https://doi.org/10.1029/2012ja017516

Gordillo-Vázquez, F. J., Passas, M., Luque, A., Sánchez, J., Velde, O., & Montanyá, J. (2018). High spectral resolution spectroscopy of sprites: A natural probe of the mesosphere. *Journal of Geophysical Research: Atmospheres*, *123*(4), 2336–2346. https://doi.org/10.1002/2017jd028126

Gordillo-Vázquez, F. J., & Pérez-Invernón, F. J. (2021). A review of the impact of transient luminous events on the atmospheric chemistry: Past, present, and future. *Atmospheric Research*, *252*, 105432. https://doi.org/10.1016/j.atmosres.2020.105432

Gordillo-Vázquez, F. J., Pérez-Invernón, F. J., Huntrieser, H., & Smith, A. (2019). Comparison of six lightning parameterizations in CAM5 and the impact on global atmospheric chemistry. *Earth and Space Science*, *6*(12), 2317–2346.

Grum, F., & Costa, L. (1976). Spectral emission of corona discharges. *Applied Optics*, *15*(1), 76–79. https://doi.org/10.1364/ao.15.000076

Hoder, T., Bonaventura, Z., Prukner, V., Gordillo-Vázquez, F. J., & Šimek, M. (2020). Emerging and expanding streamer head in low-pressure air. *Plasma Sources Science and Technology*, *29*(3), 03LT01. https://doi.org/10.1088/1361-6595/ab7087

Hoder, T., Šimek, M., Bonaventura, Z., Prukner, V., & Gordillo-Vázquez, F. J. (2016). Radially and temporally resolved electric field of positive streamers in air and modelling of the induced plasma chemistry. *Plasma Sources Science and Technology*, *25*(4), 045021. https://doi.org/10.1088/0963-0252/25/4/045021

Huang, A., Cummer, S. A., & Pu, Y. (2021). Lightning initiation from fast negative breakdown is led by positive polarity dominated streamers. *Geophysical Research Letters*, *48*, e2020GL091553. https://doi.org/10.1029/2020gl091553

Jacobson, A., Light, T., Hamlin, T., & Nemzek, R. (2013). Joint radio and optical observations of the most radio-powerful intracloud lightning discharges. *Annales Geophysicae*, *31*, 563–580. https://doi.org/10.5194/angeo-31-563-2013

Jacobson, A. R., & Heavner, M. J. (2005). Comparison of narrow bipolar events with ordinary lightning as proxies for severe convection. *Monthly Weather Review*, *133*, 1144–1154. https://doi.org/10.1175/MWR2915.1

Kuo, C., Su, H., & Hsu, R. (2015). The blue luminous events observed by ISUAL payload on board FORMOSAT-2 satellite. *Journal of Geophysical Research: Space Physics*, *120*(11), 9795–9804. https://doi.org/10.1002/2015ja021386

Kuo, C.-L., Hsu, R. R., Chen, A. B., Su, H. T., Lee, L. C., Mende, S. B., et al. (2005). Electric fields and electron energies inferred from the ISUAL recorded sprites. *Geophysical Research Letters*, *32*, L19103. https://doi.org/10.1029/2005GL023389

Le Vine, D. M. (1980). Sources of the strongest rf radiation from lightning. *Journal of Geophysical Research*, *85*(C7), 4091–4095. https://doi.org/10.1029/jc085ic07p04091

Li, D., Luque, A., Gordillo-Vázquez, F. J., Liu, F., Lu, G., Neubert, T., & Reglero, V. (2021). Blue flashes as counterparts to narrow bipolar events: The optical signal of shallow in-cloud discharges. *Journal of Geophysical Research: Atmospheres*, *126*, e2021JD035013. https://doi.org/10.1029/2021JD035013

Liu, C., Zipser, E. J., & Nesbitt, S. W. (2007). Global distribution of tropical deep convection: Different perspectives from trmm infrared and radar data. *Journal of Climate*, *20*(3), 489–503. https://doi.org/10.1175/jcli4023.1

Liu, F., Zhu, B., Lu, G., Lei, J., Shao, J., Chen, Y., et al. (2021). Meteorological and electrical conditions of two mid-latitude thunderstorms producing blue discharges. *Journal of Geophysical Research: Atmospheres*, *126*, e2020JD033648. https://doi.org/10.1029/2020JD033648

Liu, F., Zhu, B., Lu, G., Qin, Z., Lei, J., Peng, K.-M., et al. (2018). Observations of blue discharges associated with negative narrow bipolar events in active deep convection. *Geophysical Research Letters*, *45*(6), 2842–2851. https://doi.org/10.1002/2017gl076207

Liu, N., Dwyer, J. R., Tilles, J. N., Stanley, M. A., Krehbiel, P. R., Rison, W., & Wilson, J. G. (2019). Understanding the radio spectrum of thunderstorm narrow bipolar events. *Journal of Geophysical Research: Atmospheres*, *124*(17–18), 10134–10153. https://doi.org/10.1029/2019jd030439

Liu, Y., Williams, E., Li, Z., Guha, A., LaPierre, J., Stock, M., et al. (2021). Lightning enhancement in moist convection with smoke-laden air advected from Australian wildfires. *Geophysical Research Letters*, *48*(11), e2020GL092355. https://doi.org/10.1029/2020gl092355

Luque, A., Stenbaek-Nielsen, H., McHarg, M., & Haaland, R. (2016). Sprite beads and glows arising from the attachment instability in streamer channels. *Journal of Geophysical Research: Space Physics*, *121*(3), 2431–2449. https://doi.org/10.1002/2015ja022234

Lyons, W. A., Nelson, T. E., Armstrong, R. A., Pasko, V. P., & Stanley, M. A. (2003). Upward electrical discharges from thunderstorm tops. *Bulletin of the American Meteorological Society*, *84*, 445–454. https://doi.org/10.1175/BAMS-84-4-445

Malagón-Romero, A., & Luque, A. (2019). Spontaneous emergence of space stems ahead of negative leaders in lightning and long sparks. *Geophysical Research Letters*, *46*(7), 4029–4038.

Minschwaner, K., Kalnajs, L., Dubey, M., Avallone, L., Sawaengphokai, P., Edens, H., & Winn, W. (2008). Observation of enhanced ozone in an electrically active storm over Socorro, nm: Implications for ozone production from corona discharges. *Journal of Geophysical Research*, *113*(D17), D17208. https://doi.org/10.1029/2007jd009500

Montanyà, J., Fabró, F., Velde, O. V. D., March, V., Williams, E. R., Pineda, N., et al. (2016). Global distribution of winter lightning: A threat to wind turbines and aircraft. *Natural Hazards and Earth System Sciences*, *16*(6), 1465–1472. https://doi.org/10.5194/nhess-16-1465-2016

Myhre, G., Shindell, D., & Pongratz, J. (2014). Anthropogenic and natural radiative forcing. In T. Stocker (Ed.), *Climate change 2013: The physical science basis; working group 1 contribution to the fifth assessment report of the intergovernmental panel on climate change* (pp. 659–740). Cambridge: Cambridge University Press.

Neubert, T., Chanrion, O., Heumesser, M., Dimitriadou, K., Husbjerg, L., Rasmussen, I. L., & Reglero, V. (2021). Observation of the onset of a blue jet into the stratosphere. *Nature*, *589*(7842), 371–375. https://doi.org/10.1038/s41586-020-03122-6

Neubert, T., Østgaard, N., Reglero, V., Blanc, E., Chanrion, O., Oxborrow, C. A., et al. (2019). The ASIM Mission on the international space station. *Space Science Reviews*, *215*(2), 26. https://doi.org/10.1007/s11214-019-0592-z

Pérez-Invernón, F. J., Gordillo-Vázquez, F. J., Smith, A. K., Arnone, E., & Winkler, H. (2019). Global occurrence and chemical impact of stratospheric Blue Jets modeled with WACCM4. *Journal of Geophysical Research: Atmospheres*, *124*, 2841–2864. https://doi.org/10.1029/2018JD029593

Pérez-Invernón, F. J., Malagón-Romero, A., Gordillo-Vázquez, F. J., & Luque, A. (2020). The contribution of sprite streamers to the chemical composition of the mesosphere-lower thermosphere. *Geophysical Research Letters*, *47*(14), e2020GL088578. https://doi.org/10.1029/2020GL088578

Rison, W., Krehbiel, P. R., Stock, M. G., Edens, H. E., Shao, X.-M., Thomas, R. J., & Zhang, Y. (2016). Observations of narrow bipolar events reveal how lightning is initiated in thunderstorms. *Nature Communications*, *7*, 10721. https://doi.org/10.1038/ncomms10721

Schumann, U., & Huntrieser, H. (2007). The global lightning-induced nitrogen oxides source. *Atmospheric Chemistry and Physics*, *7*(14), 3823–3907. https://doi.org/10.5194/acp-7-3823-2007

Schwartz, M. J., Santee, M. L., Pumphrey, H. C., Manney, G. L., Lambert, A., Livesey, N. J., & Werner, F. (2020). Australian new year's pyrocb impact on stratospheric composition. *Geophysical Research Letters*, *47*(24), e2020GL090831. https://doi.org/10.1029/2020gl090831

Shlanta, A., & Moore, C. (1972). Ozone and point discharge measurements under thunderclouds. *Journal of Geophysical Research*, *77*(24), 4500–4510. https://doi.org/10.1029/jc077i024p04500

Simek, M. (2002). The modelling of streamer-induced emission in atmospheric pressure, pulsed positive corona discharge: N_2 second positive and NO-γ systems. *Journal of Physics D: Applied Physics D*, *35*, 1967–1980. https://doi.org/10.1088/0022-3727/35/16/311

Smith, D., Shao, X., Holden, D., Rhodes, C., Brook, M., Krehbiel, P., et al. (1999). A distinct class of isolated intracloud lightning discharges and their associated radio emissions. *Journal of Geophysical Research*, *104*(D4), 4189–4212. https://doi.org/10.1029/1998jd200045

Soler, S., Pérez-Invernón, F. J., Gordillo-Vázquez, F. J., Luque, A., Li, D., Malagón-Romero, A., et al. (2020). Blue optical observations of narrow bipolar events by ASIM suggest corona streamer activity in thunderstorms. *Journal of Geophysical Research: Atmospheres*, *125*(16), e2020JD032708. https://doi.org/10.1029/2020jd032708

Suszcynsky, D., & Heavner, M. (2003). Narrow bipolar events as indicators of thunderstorm convective strength. *Geophysical Research Letters*, *30*(17), 1879. https://doi.org/10.1029/2003gl017834

Tilles, J. N., Liu, N., Stanley, M. A., Krehbiel, P. R., Rison, W., Stock, M. G., et al. (2019). Fast negative breakdown in thunderstorms. *Nature Communications*, *10*(1), 1648. https://doi.org/10.1038/s41467-019-09621-z

Ukkonen, P., & Mäkelä, A. (2019). Evaluation of machine learning classifiers for predicting deep convection. *Journal of Advances in Modeling Earth Systems*, *11*(6), 1784–1802. https://doi.org/10.1029/2018ms001561

Wescott, E. M., Sentman, D., Osborne, D., Hampton, D., & Heavner, M. (1995). Preliminary results from the Sprites94 aircraft campaign: 2. Blue jets. *Geophysical Research Letters*, *22*, 1209–1212. https://doi.org/10.1029/95GL00582

Wescott, E. M., Sentman, D. D., Heavner, M. J., Hampton, D. L., Osborne, D. L., & Vaughan, O. H. (1996). Blue starters: Brief upward discharges from an intense Arkansas thunderstorm. *Geophysical Research Letters*, *23*, 2153–2156. https://doi.org/10.1029/96GL01969

Wescott, E. M., Sentman, D. D., Stenbaek-Nielsen, H. C., Huet, P., Heavner, M. J., & Moudry, D. R. (2001). New evidence for the brightness and ionization of blue starters and blue jets. *Journal of Geophysical Research*, *106*, 21549–21554. https://doi.org/10.1029/2000JA000429

Wiens, K. C., Hamlin, T., Harlin, J., & Suszcynsky, D. M. (2008). Relationships among narrow bipolar events,"total" lightning, and radar-inferred convective strength in Great Plains thunderstorms. *Journal of Geophysical Research*, *113*(D5), D05201. https://doi.org/10.1029/2007jd009400

Williams, E. R., Geotis, S., Renno, N., Rutledge, S., Rasmussen, E., & Rickenbach, T. (1992). A radar and electrical study of tropical "hot towers". *Journal of the Atmospheric Sciences*, *49*(15), 1386–1395. https://doi.org/10.1175/1520-0469(1992)049<1386:araeso>2.0.co;2

Zahn, A., Brenninkmeijer, C., Crutzen, P., Parrish, D., Sueper, D., Heinrich, G., & Heintzenberg, J. (2002). Electrical discharge source for tropospheric "ozone-rich transients". *Journal of Geophysical Research*, *107*(D22), 4638. https://doi.org/10.1029/2002jd002345